Fermilab Library
0 1160 0052518 2

SDC-90-00133

SDC
SOLENOIDAL DETECTOR NOTES

MEASUREMENT OF THE TOP MASS IN THE eμ CHANNEL

A. Barbaro-Galtieri, A. Bay, A. Palounek, M. Austern

December 6, 1990

SDC-90-00133
6 December 1990

Measurement of the Top Mass in the $e\mu$ Channel

A. Barbaro-Galtieri, A. Bay, A. Palounek, and M. Austern

Physics Division
Lawrence Berkeley Laboratory
1 Cyclotron Road, Berkeley, CA 94720

Abstract

We investigate the possibility of measuring the top quark mass in the SDC detector via the sequential $e\mu$ channel. In the decay sequence $t \rightarrow Wb$ we consider events with an isolated electron from top decay and a non-isolated muon from the decay of the b which is a decay product of that top. The invariant mass of these leptons can provide a top mass measurement, at 250 GeV, with an uncertainty of $\pm$ 1 GeV (stat) $\pm$ 6 GeV (sys) in one SSC year of data taking at nominal luminosity.

† This work was supported by the Director, Office of Energy Research, Office of High Energy and Nuclear Physics, Division of High Energy Physics, of the U. S. Department of Energy under Contract No. DE-AC03-76SF00098.

1. Introduction

The present top mass limit set by CDF[1] is $M(top) > 89\ GeV$. The higher luminosity of the Tevatron collider over the next few years will allow measurements to higher top masses, with discovery limits that will be dependent upon the upgrades of the machine. If the top quark mass is greater than about 200 GeV, it may fall to the SSC to discover the top and measure its properties. For a top mass of 250 GeV, $t\bar{t}$ pairs will be produced copiously at the SSC (σ=1.6 nb) and will be an important background to other physics processes.

In this note we consider measuring the top quark mass using events which contain both an isolated electron and a nonisolated muon[2] :

$$p\bar{p} \rightarrow t\bar{t} \rightarrow WbX$$

with

$$W \rightarrow e\nu \text{ (isolated electron)}$$

and

$$b \rightarrow \mu X \text{ (muon in a jet, or nonisolated).}$$

This topology is called the "sequential e-μ" topology, because the e and the μ come from subsequent decays of the W and the b from the same top quark. The variable that appears to be most sensitive to the top mass is $M(e\mu)$, the invariant mass of the two leptons.

Section 2 describes event generation and detector simulation, section 3 the event selection, and section 4 the background. Finally, section 5 describes the results, section 6 the systematic errors, and section 7 gives the conclusions.

2. Event Generation and Detector Simulation

This study uses ISAJET 6.31[3] to generate samples of $t\bar{t}$ events at the SSC energy of 40 TeV. We have generated a total of 5.5 million events at five top masses between 220 and 280 GeV and top p_t ranging from 4 GeV/c to 3000 GeV/c. For the 250 GeV mass we also generated a sample in the p_t range 5-1000 GeV/c and two other samples for determining the systematic uncertainty on the mass determination (see Section 6). Table 1 shows the number of events generated, event cross section and integrated luminosity for the 250 GeV top runs. Table 2 contains the same information for the other mass values. Tables 1 and 2 also list the number of events which pass our cuts for this analysis, as described in Section 3 below.

The electrons and muons pass through the standard SDC four-vector smearing routines[4] which correspond to the geometry of the descoped SDC detector, with a nominal electromagnetic calorimeter resolution

$$\frac{\Delta E}{E} = \frac{0.15}{\sqrt{E}} \oplus 0.01 \qquad |\eta| < 3, \tag{1}$$

and muon resolution

$$(\frac{\Delta p_t}{p_t})^{-2} = \frac{1}{(0.0053)^2 + 0.00026(p_t)^2} + \frac{1}{(0.16\sqrt{\sin\theta})^2 + (0.0000545 p_t)^2} \qquad |\eta| < 1.7$$

$$\frac{\Delta p_t}{p_t} = 0.11\sqrt{\cos\theta} \oplus 0.000075\frac{\cos^2\theta}{\sin\theta}p_t \qquad 1.7 < |\eta| < 2.5 \tag{2}$$

where $\oplus$ means that the two terms were added in quadrature. We have assumed an 85% efficiency in detecting and identifying each of the two leptons. For the final results we have normalized the generated samples to an integrated luminosity of 10000 pb^{-1}, or one nominal SSC year.

3. Event Selection

For this analysis we have to apply requirements on the data so that we select preferentially events coming from the sequence

$$t \rightarrow Wb$$

with

$$W \rightarrow e\nu$$

and

$$b \rightarrow \mu X$$

Figure [1] shows the E_T distribution of the electron from the W, and figure [2] shows the p_t distribution of the μ from the bottom decay. Notice that both plots start at 15 GeV/c due to an arbitrary 15 GeV/c cut in the ISAJET sample that we retained for further analysis. In top events electrons and muons can come also from subsequent decays of charm quarks, as shown in Figure [3]. Leptons from charm, however, will tend to be of lower momentum than the ones from top and bottom. In addition, leptons from top will be isolated, whereas those from bottom and charm will be nonisolated. Figure [4] shows examples of isolated and nonisolated leptons in heavy quark decays.

In this study we assume the use of events from an electron inclusive trigger with $E_T >$ 35 GeV and assume that the trigger becomes fully efficient at 40 GeV. In addition, the electron is required to be isolated. To study the isolation of electrons from top decay we calculate the vector sum of the transverse energy of all particles (except for neutrinos) in a cone about the electron direction. Defining $\Delta R = \sqrt{d\eta^2 + d\phi^2}$, we show in Figure [5] the distribution of E_T in a cone of $\Delta R = 0.2$ around the electron direction. This shows that a requirement of $E_T < 4$ GeV removes only 9% of the sample while insuring that the electron is truly isolated. Therefore, for the electron we require:

- $E_T > 40$ GeV
- $|\eta| < 3$
- $E_T(\text{cone of } \Delta R = .2) < 4$ GeV

A few comments on electron isolation follow. In Figure [5] we have used the full sample, the run with a top p_t range of 5 to 1000 GeV/c. The electron E_T is required to be $E_T > 40$ GeV. Figure [6] shows the E_T distribution in a cone of $\Delta R = 0.2$ for electrons from true top decays, for different top p_t bins. Note that these data are not normalized relative to one another. We point out that for electron $E_T > 40$ GeV, the energy in the cone is almost independent of top p_t. Figure [7] shows the E_T distribution for a cone of $\Delta R = 0.4$ for the full sample.

We now turn to the muon requirements. First we look at the isolation. Figure [8] shows E_T in a cone of $\Delta R = 0.4$ around the muon direction for the complete top sample (p_t = 5-1000 GeV/c). The muon is required to be a decay product of a b coming from top decay. A cut at 20 GeV removes only 6% of this sample, and would include a very small fraction of muons from top decays (see Figure [7]). Therefore, we impose the following requirements on the muon from the associated b decay:

- opposite sign from the electron,
- $p_t > 20$ GeV/c,
- $|\eta| < 2.5$
- $E_T(\text{cone of } \Delta R = 0.4) > 20$ GeV

The p_t cut at 20 GeV/c reduces background from charm decays and enhances the region of phase space where the muon p_t carries information about the top mass. Figure [9] shows the E_T in a cone of $\Delta R = 0.4$ for muons from the decay of a b from a top for four different bins of top p_t. We notice that for higher top p_t the distributions are broader and peak at higher E_T , as expected for increased jet activity in the event.

Figure [10] shows some properties of the $e\mu$ pairs which come from real "sequential top decays": the ϕ, η and R separation of the two leptons and the $p_t(e\mu)$ for the sample selected with the above cuts. Figure [11] shows the same distributions for all $e\mu$ combinations. Clearly the $\Delta\phi$ distribution is very different from that of Figure [10]. It shows a peak at 180° which is likely to come from charm contamination (see Figure [3]). The $\Delta\eta$ distributions are very similar whereas the ΔR distributions reflect the difference in the $\Delta\phi$ distributions. To maximize the probability that the e and μ both come from decays associated with the same top quark, that is, to reduce charm background from the other top (see Fig. [3]), we require that both leptons be in the same hemisphere. After comparing figures [10] and [11] we impose a requirement of $\Delta\phi < 80°$. The $\Delta\phi$ cut removes 51% of good $e\mu$ combinations, but it also removes 63% of combinatoric background, giving an $e\mu$ sample purity of 77%.

We now compare the $p_t(e\mu)$ distributions for real top events and for the sequential $e\mu$ sample we have obtained with the above selection. These are shown in figures [10d] and [11d]. For both plots we have already applied the $\Delta\phi$ cut. The distributions are quite similar. To maximize sensitivity to the top quark mass we add the additional requirement $p_t(e\mu) > 120\ GeV/c$ (see section 5) and obtain the $e\mu$ separations shown in Figures [12a-c]. Finally, Figure [12d] shows the $e\mu$ invariant mass for all combinations after all the cuts above.

The comparison between the $M(e\mu)$ obtained with the real "sequential top decays" and the one obtained by all $e\mu$ combinations is shown in Figure [13]. The distributions are remarkably similar with a peak position at the same value, which shows that the remaining charm background is small.

4. Background from other processes

The requirements on the electron and muon discussed above serve to reduce the background from wrong $e\mu$ combinations in the $t\bar{t}$ events. Backgrounds from other processes are expected to be small. The most significant ones are due to:

- WW production could be a source of isolated e from one W and nonisolated μ from the hadronic decay of the other W;

- WZ production could give an isolated e from the W and a nonisolated μ from the hadronic decay of the Z.

- $Wb\bar{b}$ production, where $W \rightarrow e^+\nu$ and $\bar{b} \rightarrow \mu^-$ could fake our event topology.

We estimate[5] that the background from processes such as WW ($\sigma = 240\ pb$) , WZ ($\sigma = 80\ pb$) is much smaller than that from the $Wb\bar{b}$ channel. In order to estimate this background we invoked the ISALEP option of ISAJET 6.36 [3] for $W + jet$ production. Accepting events with any $p_t(W)$ above 0.1 GeV, we obtain a cross section of 5.6 nb for $Wb\bar{b}$ with a lepton with $p_t > 15\ GeV$ and a $b\bar{b}$ pair in the final state. Requiring bottom decay to muons and applying the cuts used to select "sequential $e\mu$ events," we remove many but not all of the candidates from $Wb\bar{b}$ events: 13 events are left in 320 pb^{-1}. Figure [14] shows the M($e\mu$) for these events, compared with the distribution for the sequential $e\mu$; the $Wb\bar{b}$ contamination corresponds to 3% of the signal. Preliminary calculations with VECBOS[6] with slightly different cuts, gave an 8% estimate for the background. This is not surprising as VECBOS uses exact matrix elements whereas ISAJET's calculations are approximate. Still, the 8% background will not affect the results presented here.

All of the background estimates are subject to uncertainties in the evaluation of the cross sections for these processes.

5. Results

Figure [15] shows the comparison of the $e\mu$ invariant mass as obtained with top masses of 220 and 250 GeV. The gaussian fits shown describe the data quite well and determine the peak of the distributions with a good accuracy. The two distributions are clearly different. Table 3 and figure [16] show the fit results for five top masses between 220 and 280 GeV. They show a linear dependence of $M(e\mu)$ on the top mass. Using a cut of 120 GeV/c on the p_t of the $e\mu$ pair, for $M(top) = 250\ GeV$ the gaussian fit gives:

$$M(e\mu) = 86.7 \pm 0.24\ GeV \tag{3}$$

The fit for the five masses shown in Figure [16] gives the relation:

$$dM(e\mu) = (0.288 \pm 0.005) dM(top) \tag{4}$$

which gives:

$$M(top) = 250 \pm 1 \text{ (stat)} \tag{5}$$

To maximize the sensitivity to the top quark mass, we have required that the p_t of the combined $e\mu$ system be greater than 120 GeV. Figure [17] shows the p_t distribution of all $e\mu$ pairs which pass the electron and muon requirements discussed in section 3 for $M(top) = 250\ GeV$. The distribution peaks at 60 GeV/c, and tapers off quickly; a cut at 120 GeV/c reduces the sample considerably. We have studied the variation of M($e\mu$) with this cut. The results for $p_t(e\mu) > 80\ GeV/c$ and $p_t(e\mu) > 160\ GeV/c$ are shown also in Figure [16] and Table 3. We see that the linear dependence persists for other $p_t(e\mu)$ cuts and that this dependence is more pronounced for the higher p_t cuts.

Table 3 summarizes the results. It shows the number of events expected in an SSC year and the slope of the $p_t(e\mu)$ dependence at each of the masses and p_t cuts. Cutting at $p_t(e\mu) > 120\ GeV/c$ yields both an adequate sensitivity to the top mass and sufficient events for a top mass determination.

6. Uncertainties in the Mass Measurement

The error on the top mass measurement with this method is likely to be dominated by systematic uncertainties due to uncertainties in the physics assumptions. We consider errors arising from uncertainties in the b fragmentation function and the top p_t distribution.

6.1 b fragmentation effects

The b fragmentation function controls the μ momentum distribution. Heavy quark fragmentation in ISAJET is parametrized with the Peterson fragmentation function.[7] We have run ISAJET changing the parameter ϵ of the Peterson function by one standard deviation as measured by ALEPH:[8]

$$\epsilon = 0.006\ ^{+0.004}_{-0.003} \tag{6}$$

This corresponds to changing[9] the ISAJET parameter XGEN to 0.167, since the default value of 0.5 corresponds to $\epsilon = 0.01$. The lower points at $M(top) = 250\ GeV$ in Figure [16] correspond to the lower value of ϵ. The two runs give a range of $\pm 3\ GeV$ on the top mass due to uncertainty in the b fragmentation function.

6.2 dependence on the top production mechanism

We have also studied the dependence of the measured $M(e\mu)$ on the top p_t distribution. We find this dependence to be rather strong.

Figure [18] shows, for $M(top) = 250\ GeV$, the $p_t(top)$ distributions obtained in ISAJET for the six different p_t bins used for the runs of Table 1. We combine these runs, properly weighted, to obtain the top p_t distribution shown in Figure [20] as a solid curve. We then take ranges of $p_t(top)$ and plot the $e\mu$ invariant mass. Figures [19a-d] show the $M(e\mu)$ distributions for several $p_t(top)$ ranges. We fit each of these distributions and show in Figure [21] the fitted values of $M(e\mu)$ as a function of $p_t(top)$. There is a clear dependence of $M(e\mu)$ on $p_t(top)$. The values of $M(top)$ corresponding to each of these $M(e\mu)$ values are shown in Table 4. The results show that the top mass determination depends on the top p_t distribution, i.e, on the knowledge of the top production mechanism.

With ISAJET we have generated only events where the $t\bar{t}$ pairs were produced directly from quarks and gluons. There are other processes, like gluon splitting (a gluon giving a $t\bar{t}$ pair), and flavor excitation which can produce a different $p_t(top)$ distribution. This is also the case for Wt production. Figure [22] shows the Wt cross section compared to the $t\bar{t}$ cross section as a function of the top mass at LHC energy[10]. It shows that at $M(top) = 250\ GeV$, this process is nonnegligible. This will be the case at SSC also. In order to generate a different top p_t spectrum, we have changed the Q^2 scale in ISAJET by a factor of 3, thus altering the initial state radiation. Figure [20] shows the $p_t(top)$ spectrum before (solid) and after (dashed) changing the Q^2 scale.

The different p_t spectra give a difference in $M(top)$ of 5 GeV and we take this to be the systematic error due to uncertainty on the top production mechanism.

6.3 Total systematic error

Adding these uncertainties in quadrature, we expect to determine the top mass at 250 GeV with uncertainty ± 1 (stat) ± 6 (sys) for one year of running at the SSC design luminosity. Both the systematics uncertainties we have considered can be studied when the SSC data are on hand. Hopefully tuning the Monte Carlo to the data can reduce the uncertainty considerably.

7. Conclusions

The technique of selecting isolated electrons and nonisolated muons which come from decays of the same top quark works well. Using a cut of 120 GeV/c on the p_t of the $e\mu$ pair, we find:

$$M(top) = 250 \pm 1 \text{ (stat)} \pm 6 \text{ (sys)} \; GeV \tag{7}$$

for one year of SSC running at the design luminosity. The systematic uncertainty considered here can be reduced by detailed studies of the data, when they become available.

REFERENCES

1. K. Sliwa (CDF Collaboration), "A New limit on the mass of the top quark", Proceedings of the XXVth Rencontres de Moriond, Hadronic Session, Les Arcs, Savoie, France (March 1990). See also G.P.Yeh, Proceedings of Les Rencontres de Physique de La Vallee D'Aoste, La Thuile, Italy, p. 451 (March,1990).
2. Larry Nodulman has presented results on a similar method at the Snowmass Workshop (1990).
3. F. Paige and S. D. Protopopescu, "ISAJET - A Monte Carlo Generator for *p-p* and $\bar{p}$-*p* Reactions," Brookhaven National Laboratory Report BNL 38034 (1986).
4. Ian Hinchliffe, "Resolution Parametrizations for the LoI," SDC Report SDC-90-00100 (September 1990).
5. E. Eichten, I. Hinchliffe, K. Lane, and C. Quigg, Rev. Mod. Phys., **56**, 579 (1984).
6. W. Giele, S. A. Berends, H. Kuijf, B. Tausk, University of Leiden, paper in preparation (1990). This calculation was done after the LOI was completed. We thank Bob Drucker for running the program for us.
7. C. Peterson, D.Schlatter, I. Schmitt and P.Z.Zervas, Phys. Rev. **D27**, 105 (1983).
8. D. Decamp *et al.*, (ALEPH Collaboration) "Heavy flavour production in Z decays," Phys. Lett. **B244**, 551 (1990).
9. Study made by Ken Ragan for the CDF *b* studies (private communication).
10. R. Phillips, P.Z. Zervas, Zunft, plot shown by Daniel Denegri at the LHC Aachen workshop (October 1990).

Top Mass (GeV)	p_t Range (GeV/c)	Events Gen (thousands)	Event σ (nb)	Integrated $\mathcal{L}$ (pb^{-1})	sequential $e\mu$ Events (one SSCY)
250	4-50	70	0.102	1908	262
250	50-150	300	0.585	1420	1485
250	150-300	450	0.646	1503	6030
250	300-600	150	0.243	1710	8233
250	600-1000	200	0.021	26000	1404
250	1000-3000	50	0.002	64500	131
total	4-3000	1220	1.599		17545
250	5-1000	753	1.594	1314	19620
250 (b frag)	50-1000	300	1.49	1541	18450
250 ($p_t(top)$)	50-1000	245	1.489	456	14760

Table 1: The number of events generated, event cross section, effective integrated luminosity, and number of sequential $e\mu$ events normalized to one SSC year at top mass 250 GeV and several top p_t ranges. The last two rows give these values for the $p_t(top)$ dependence and b fragmentation study samples. The fluctuation in the total number of sequential $e\mu$ events over the last four rows reflects the fact that a luminosity corresponding to a fraction of an SSC year has been generated.

Top Mass (GeV)	p_t Range (GeV/c)	Events Gen (thousands)	Event σ (nb)	Integrated $\mathcal{L}$ (pb^{-1})	sequential $e\mu$ Events (one SSCY)
220	4-50	100	0.220	1282	281
220	50-150	662	1.150	1596	2539
220	150-300	500	1.025	1349	9445
220	300-600	200	0.305	1819	11134
220	600-3000	200	0.025	22185	1499
total	4-3000	1662	2.725		24898
235	4-50	100	0.147	1888	281
235	50-150	200	0.815	680	2343
235	150-300	200	0.813	681	7742
235	300-600	200	0.273	2026	9978
235	600-1000	100	0.022	12500	746
235	1000-3000	50	0.002	63860	127
total	4-3000	850	2.072		21217
265	4-50	100	0.072	3867	253
265	50-150	300	0.427	1947	1345
265	150-300	250	0.516	1342	4189
265	300-600	200	0.216	2563	7866
265	600-3000	100	0.023	12230	1542
total	4-3000	950	1.233		15195
280	4-50	100	0.051	5403	194
280	50-150	200	0.314	1760	1330
280	150-300	200	0.413	1345	2045
280	300-600	200	0.192	2886	3378
280	600-3000	100	0.022	12774	1540
total	4-3000	800	0.992		8487

Table 2: The number of events generated, event cross section, effective integrated luminosity, and number of sequential $e\mu$ events normalized to one SSC year for several top mass and top p_t ranges.

$p_t(e\mu)$ cut (GeV/c)	Top Mass (GeV)	Events Expected (one SSCY)	Calculated $M(e\mu)$ (GeV)	Slope
80	220	43810	70.45 ± .15	
80	235	34886	75.60 ± .16	
80	250	29837	78.60 ± .20	0.273 ± .004
80	265	24073	84.56 ± .23	
80	280	12920	85.26 ± .32	
120	220	24616	77.86 ± .18	
120	235	20920	83.92 ± .18	
120	250	17610	86.69 ± .24	0.288 ± .005
120	265	15234	92.47 ± .26	
120	280	8285	94.11 ± .36	
160	220	12584	83.54 ± .23	
160	235	10274	91.04 ± .24	
160	250	9993	93.56 ± .31	0.312 ± .006
160	265	8986	100.19 ± .31	
160	280	4896	100.93 ± .40	

Table 3: The number of sequential $e\mu$ events expected in one SSC year (10000 pb^{-1}) and the calculated $e\mu$ invariant mass for three values of the $p_t(e\mu)$ cut and five top quark masses. The final column shows the slope of the linear dependence of $M(e\mu)$ on $M(top)$, as is shown by the fitted line in Figure [16].

p_t Range (GeV/c)	$M(e\mu)$ (GeV)	$M(top)$ (GeV)
50-150	84.3 ± 5.1	240 ± 18
150-250	90.2 ± 1.7	260 ± 6
250-350	91.3 ± 1.1	264 ± 4
350-500	83.0 ± 1.0	235 ± 4
500-650	78.8 ± 1.0	221 ± 3
650-1000	76.7 ± 1.0	213 ± 3

Table 4: The fitted invariant mass $M(e\mu)$ for samples with different $p_t(top)$ ranges. All the sequential $e\mu$ cuts have been applied, as has the requirement that $p_t(e\mu) > 120\ GeV$. The calculated $M(top)$ in the final column assumes the straight line fit for the $p_t(e\mu) > 120\ GeV$ sample in Figure [16].

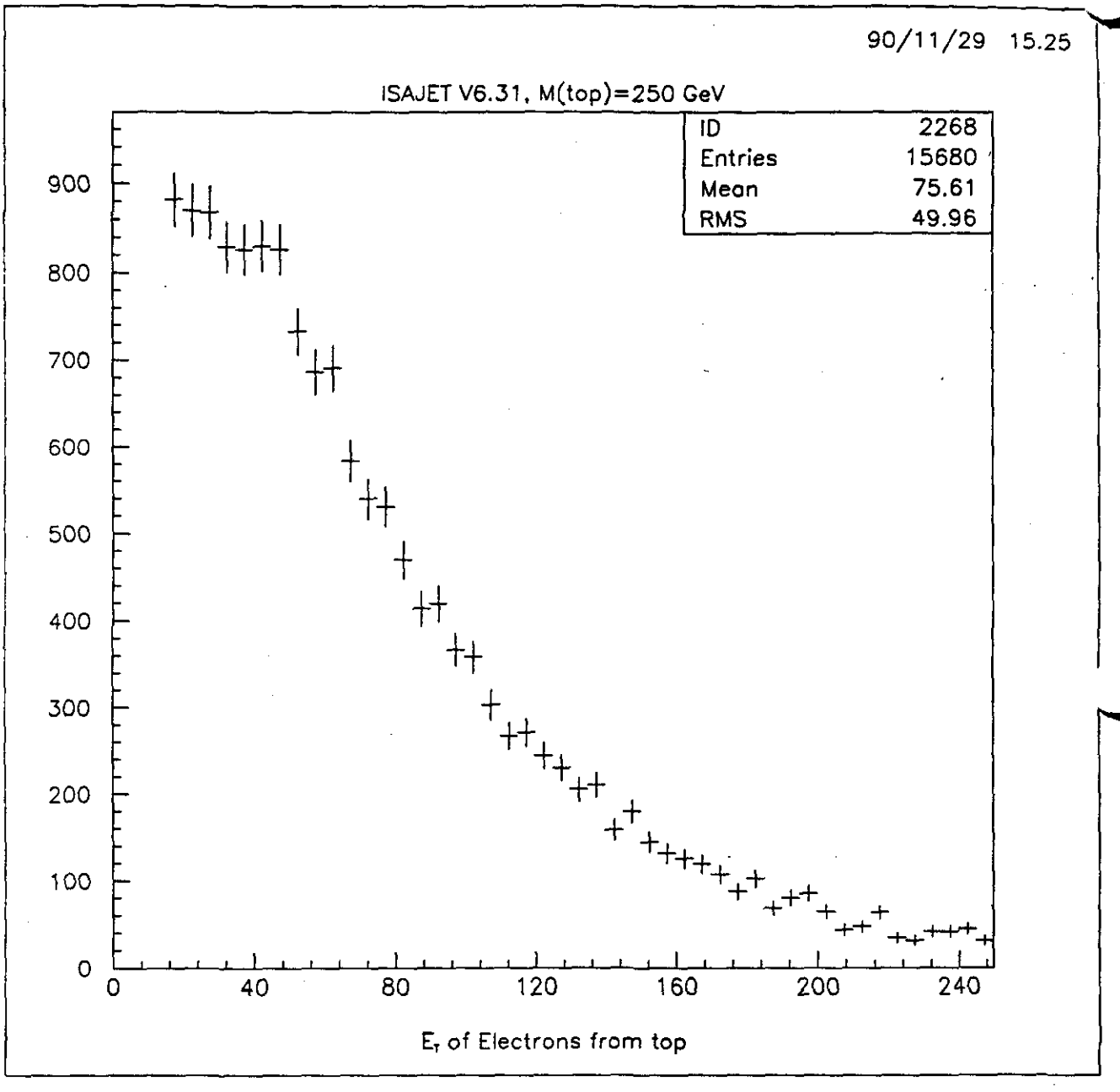

Figure 1) The E_T distribution of electrons from decay of the W from top decay.

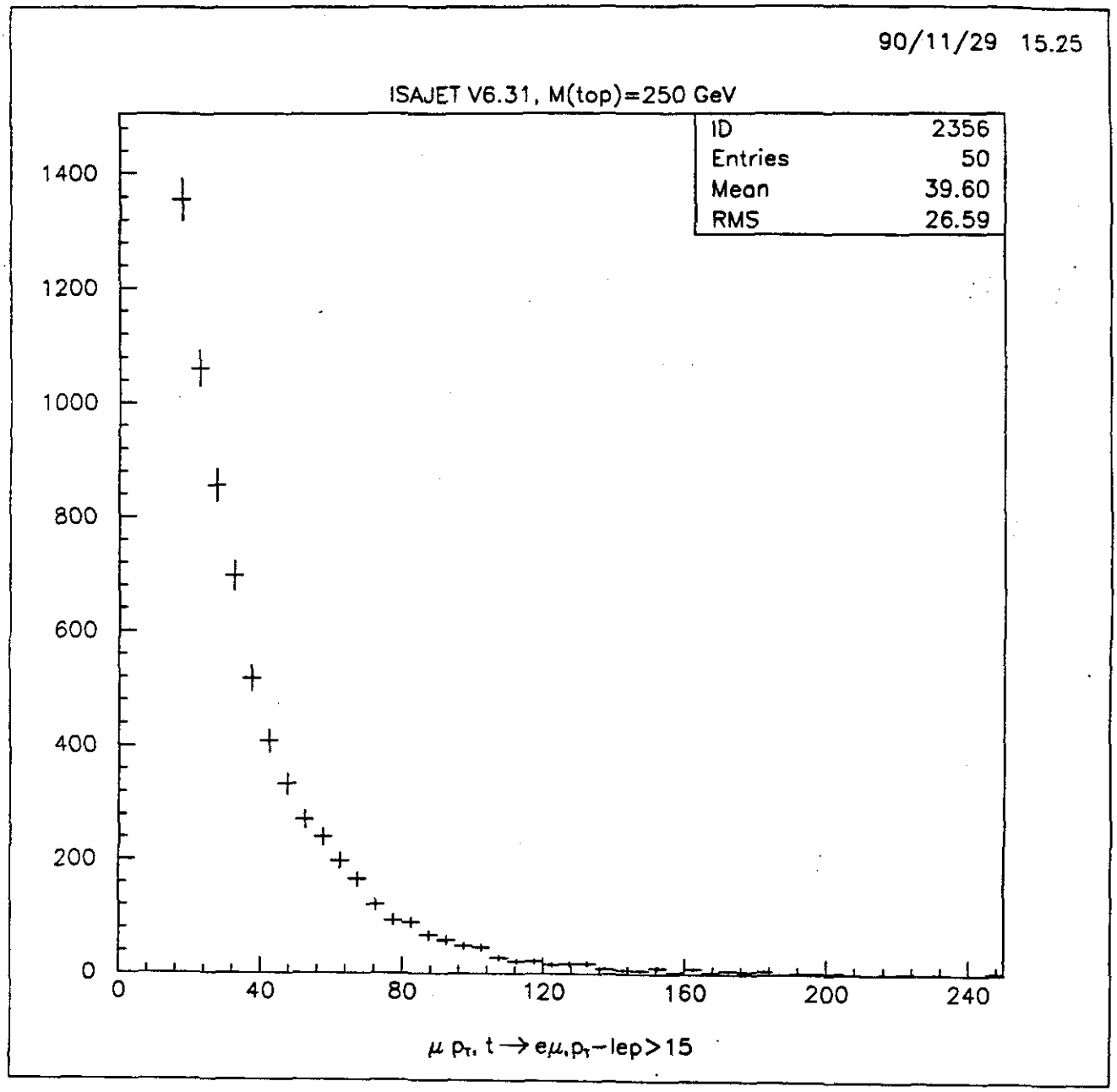

Figure 2) The p_t distribution of μs from decays of b from top decays.

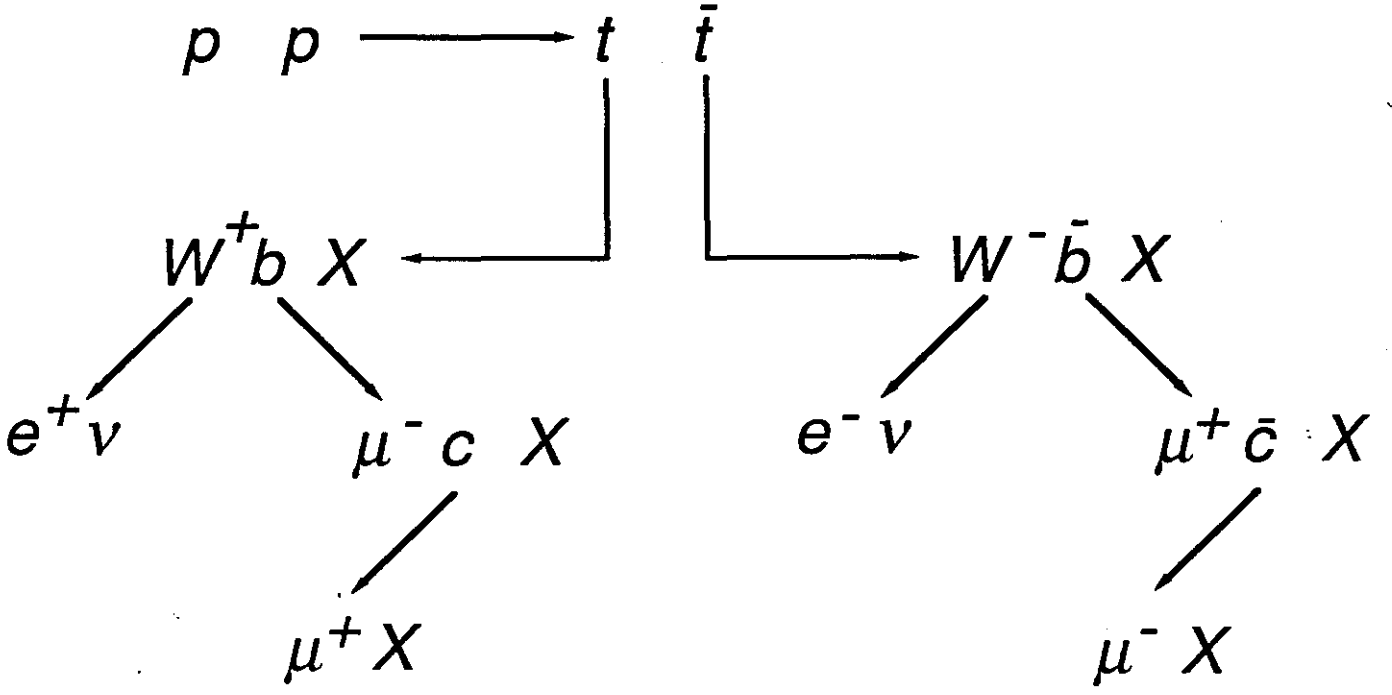

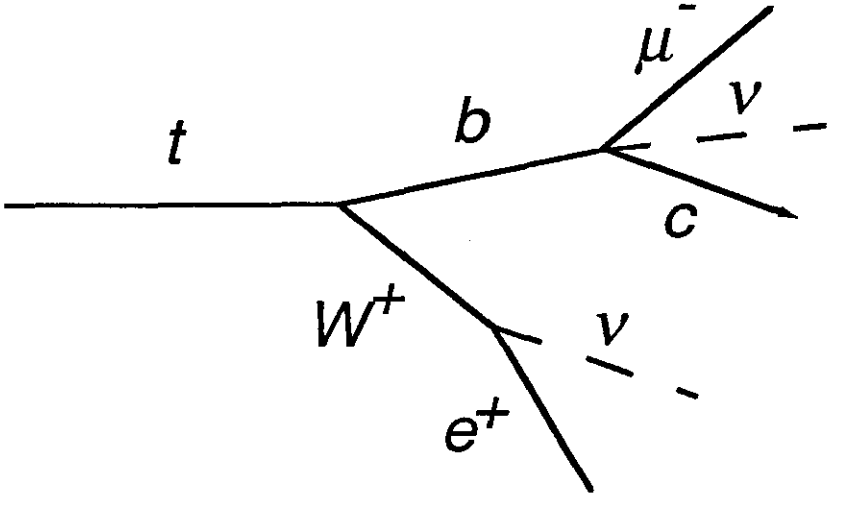

Figure 3) Schematic of top production and decay into leptons.

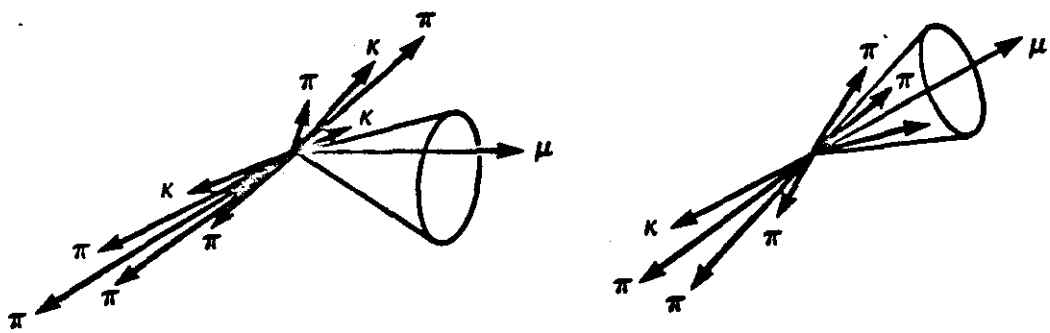

XBL 8712-5802

Figure 4) An example of isolated and non-isolated leptons in an event.

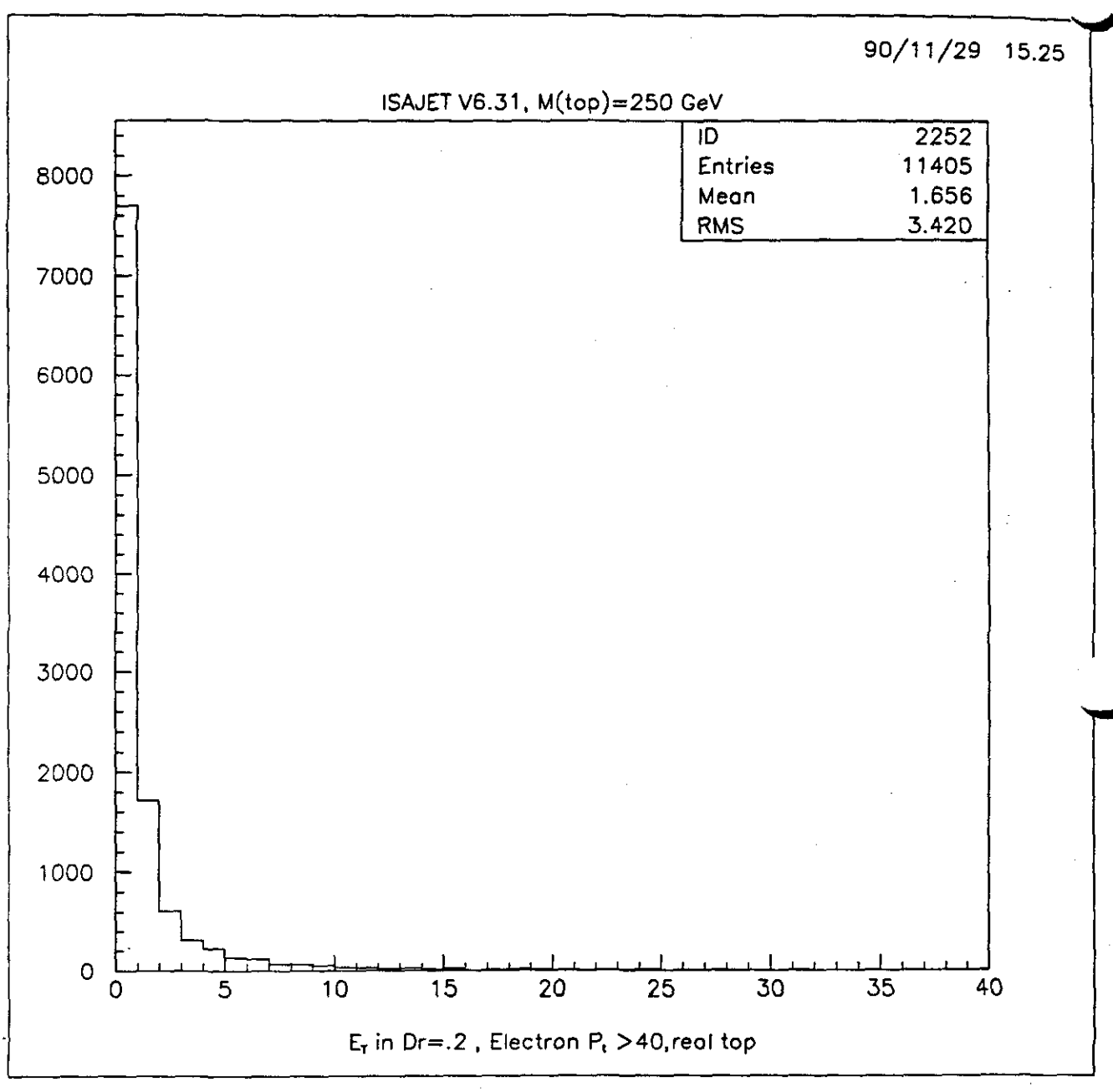

Figure 5) Distribution of transverse energy/(1 GeV) in a cone of $\Delta R = 0.2$ around the electron direction for top decay electrons with $E_T > 40$ GeV. The complete top sample was used, i.e., the run with p_t range 5-1000 GeV/c.

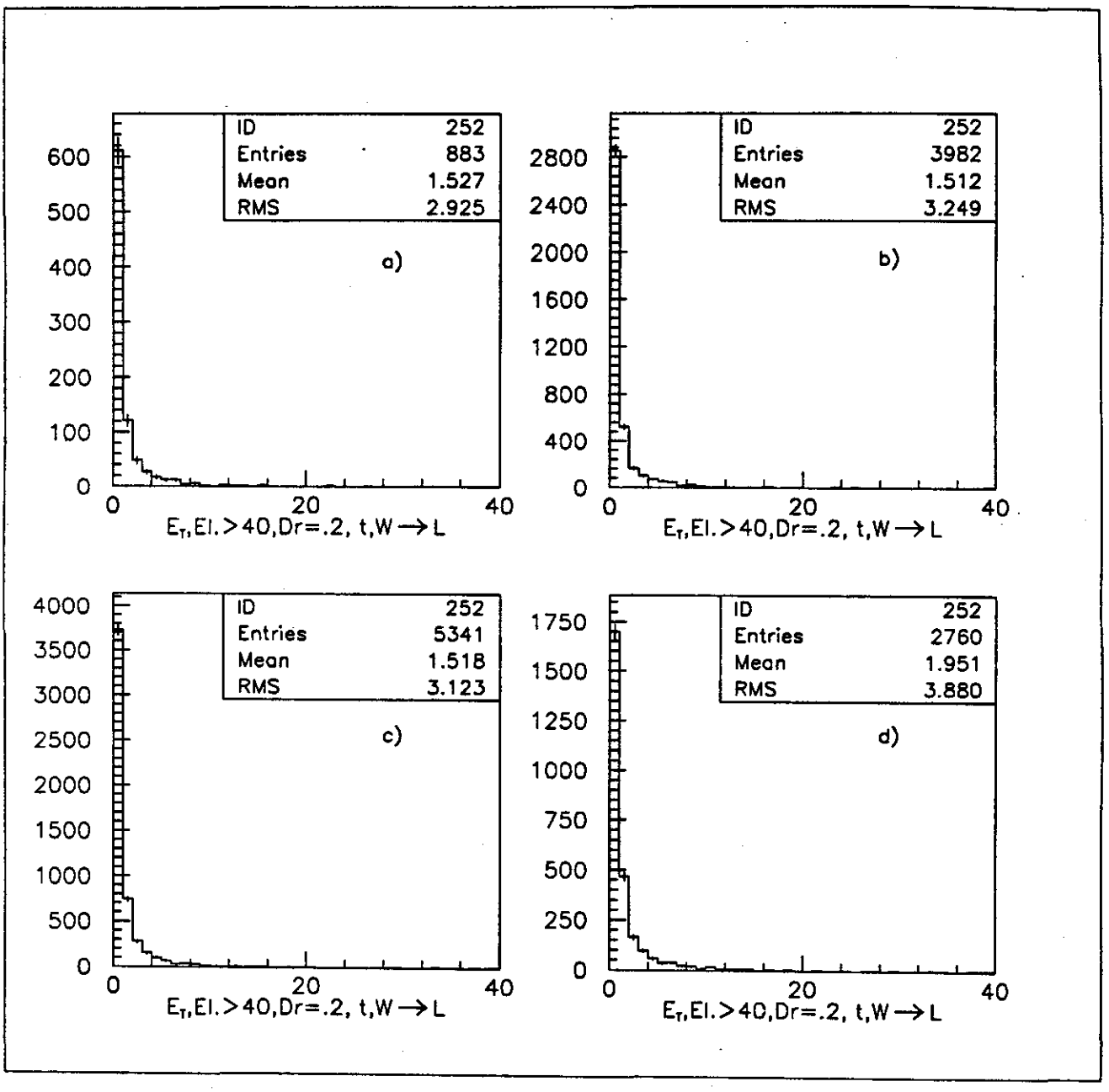

Figure 6) Distribution of transverse energy in a cone of $\Delta R = 0.2$ around the electron from a true top decay for different p_t ranges of the top produced: a) $4 < p_t(\text{top}) < 50\ GeV/c$,b) $50 < p_t(\text{top}) < 150\ GeV/c$, c) $150 < p_t(\text{top}) < 300\ GeV/c$, and d) $300 < p_t(\text{top}) < 600\ GeV/c$. $M(top) = 250\ GeV$ in all cases, and the electrons are required to have $E_T > 40\ GeV$.

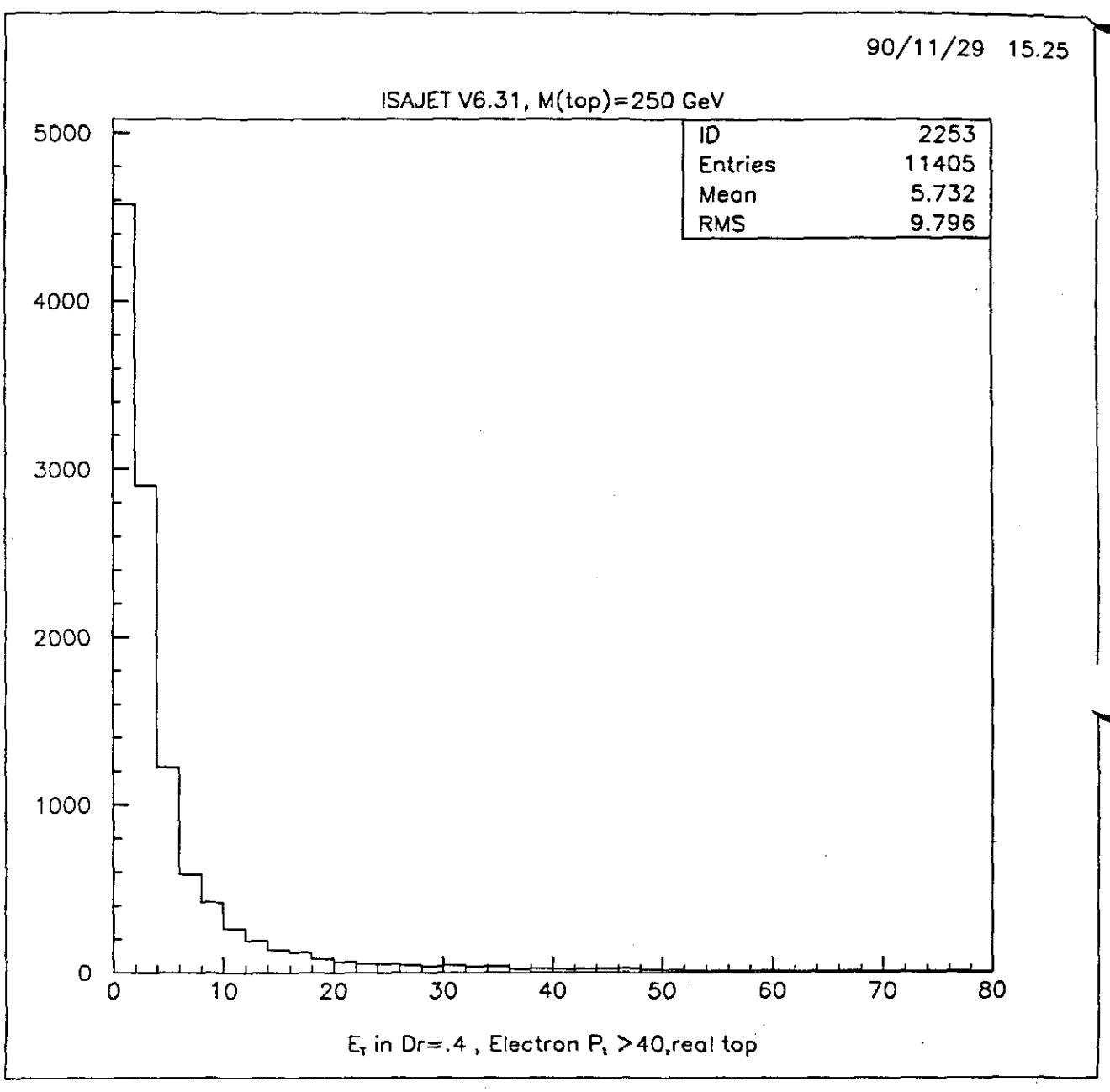

Figure 7) Same as Figure [5] above, but with $\Delta R = 0.4$.

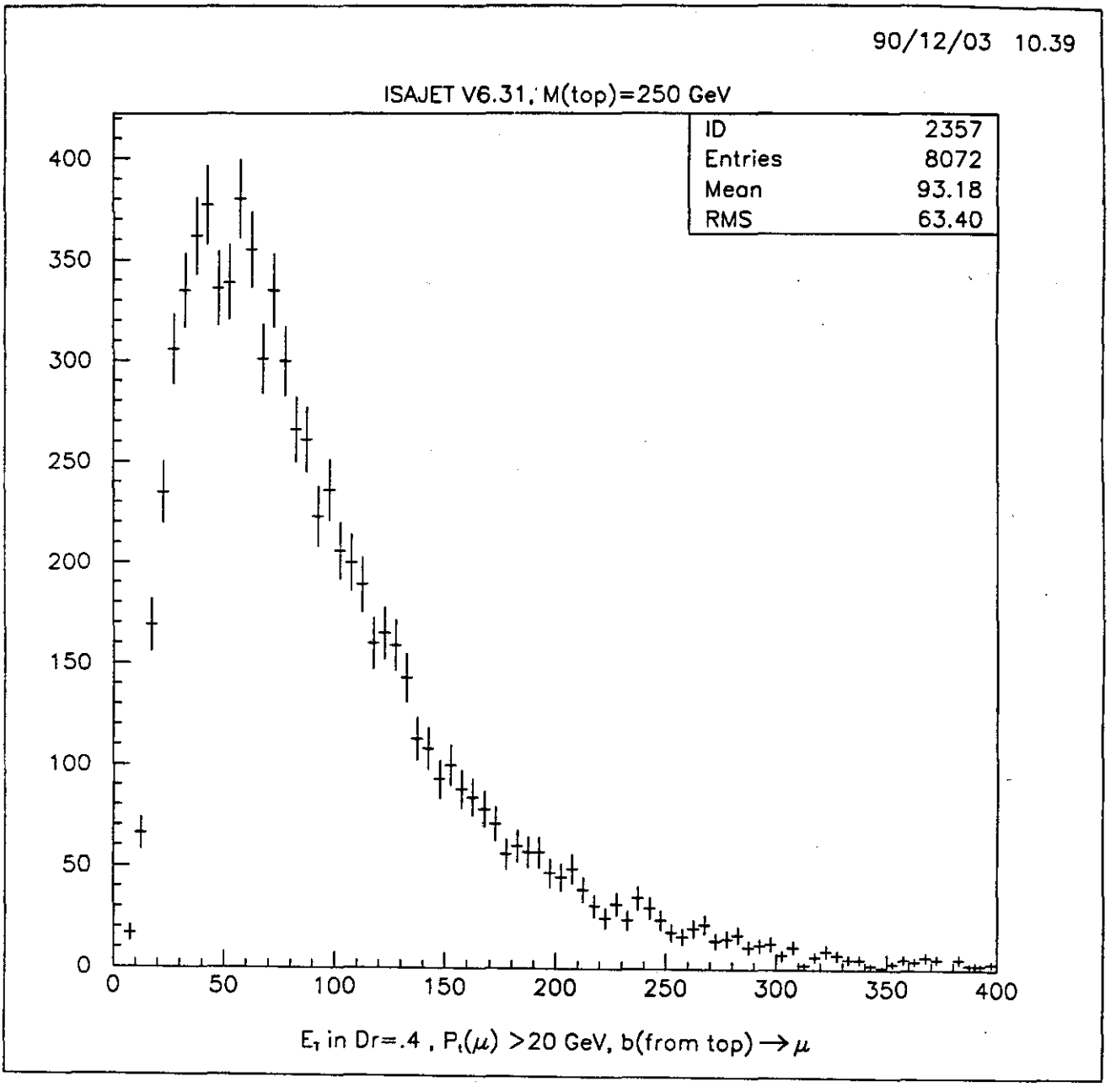

Figure 8) Distribution of transverse energy/(5 GeV) in a cone of $\Delta R = 0.4$ around the muon direction for muons coming from a b which is a top decay product. Events for the whole top sample are shown. Each event must have an e with $E_T > 40\ GeV$ and a μ with $p_t > 20\ GeV/c$.

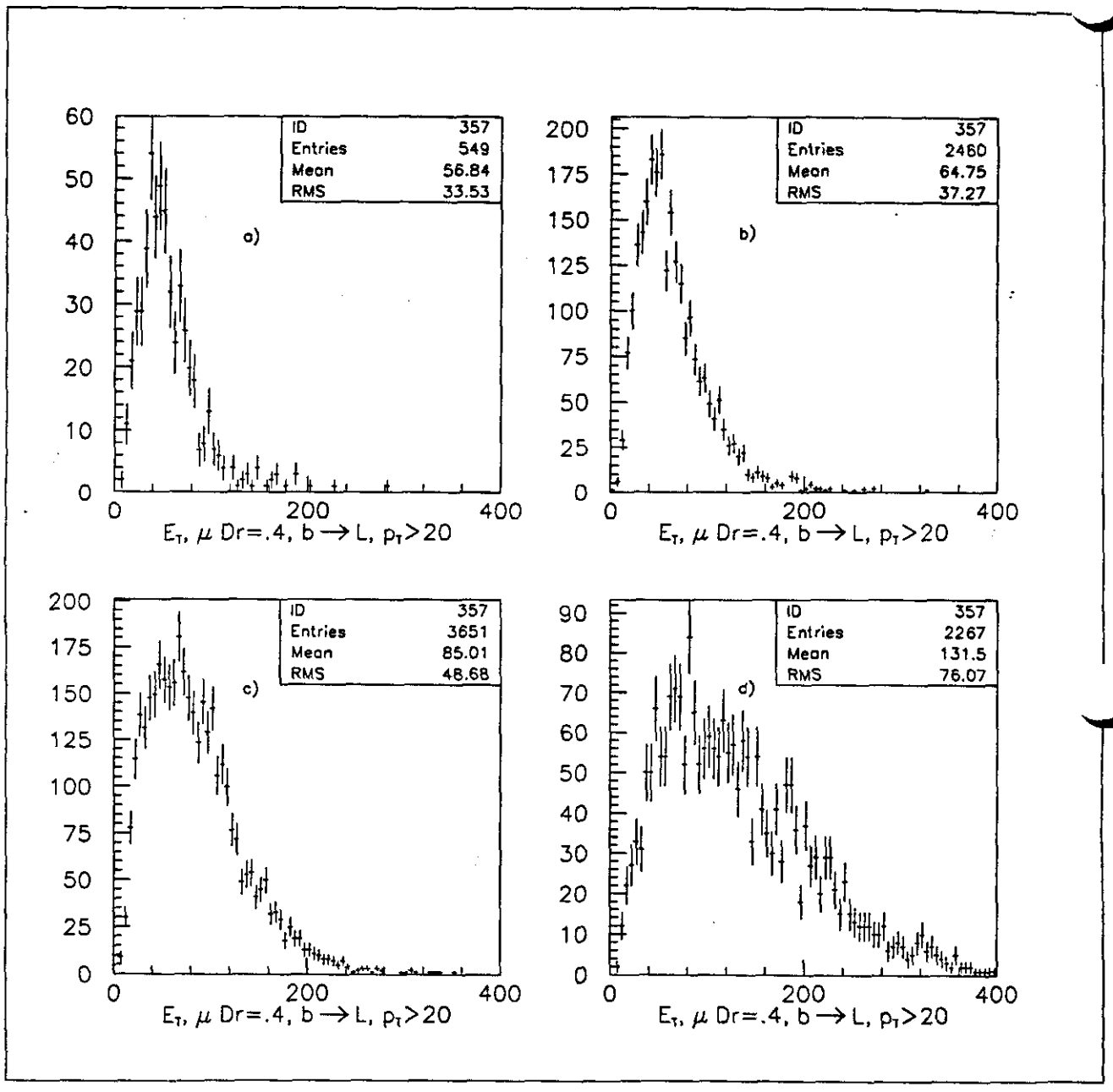

Figure 9) Distribution of transverse energy in a cone of $\Delta R = 0.4$ around the muon direction for muons coming from a b decay: a) $4 < p_t(\text{top}) < 50\ GeV/c$; b) $50 < p_t(\text{top}) < 150\ GeV/c$; c) $150 < p_t(\text{top}) < 300\ GeV/c$; d) $300 < p_t(\text{top}) < 600\ GeV/c$. $M_{top} = 250\ GeV$ in all cases, and the lepton cuts are as in Figure [8].

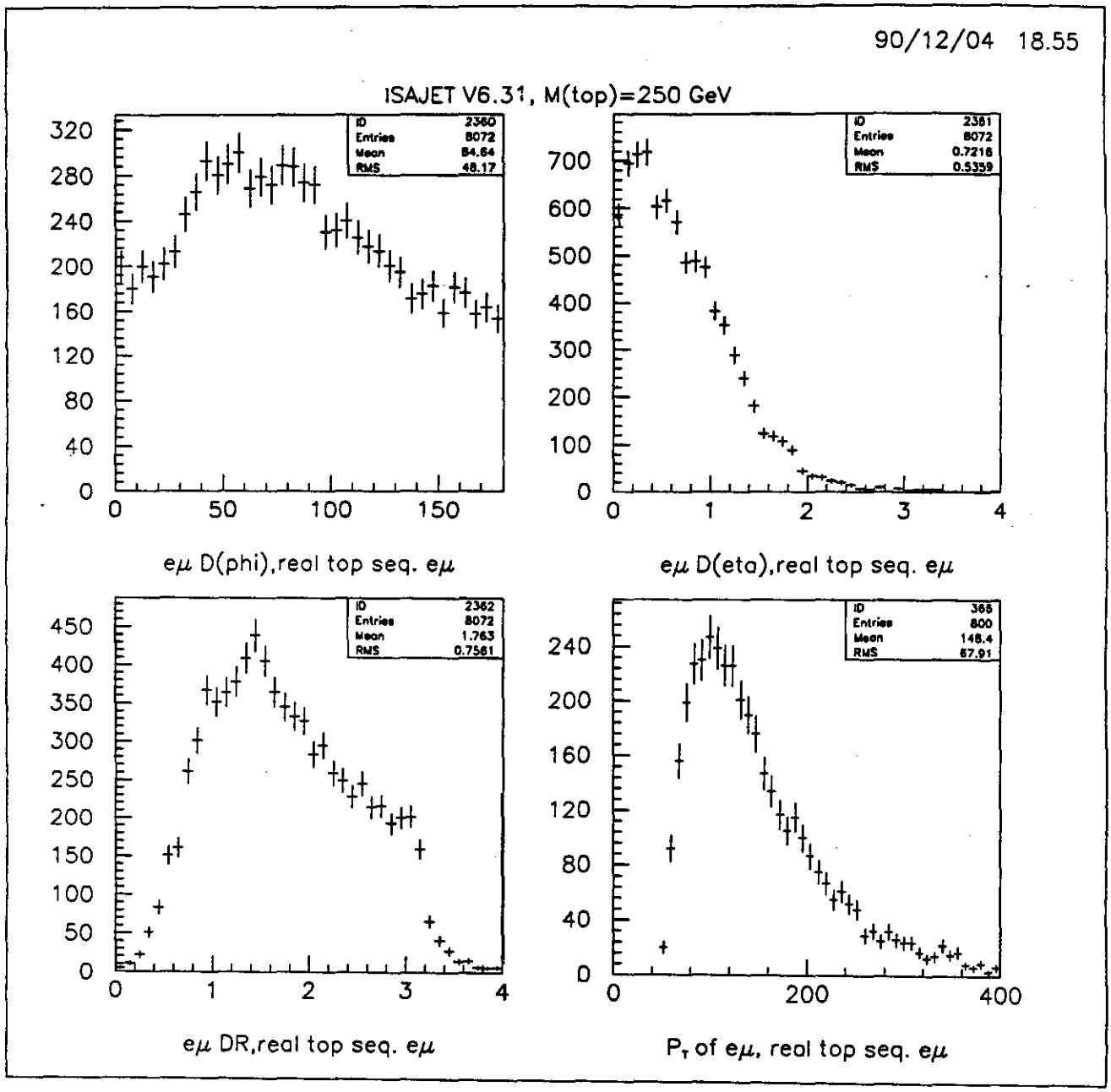

Figure 10) Properties of $e\mu$ pairs which come from true sequential top decays: a) $\Delta\phi$; b) $\Delta\eta$; c) ΔR; and d) the p_t distribution of the $e\mu$ pair. Lepton cuts are as in Figure [8], and in d) we have added the $\Delta\phi > 80$ ° cut.

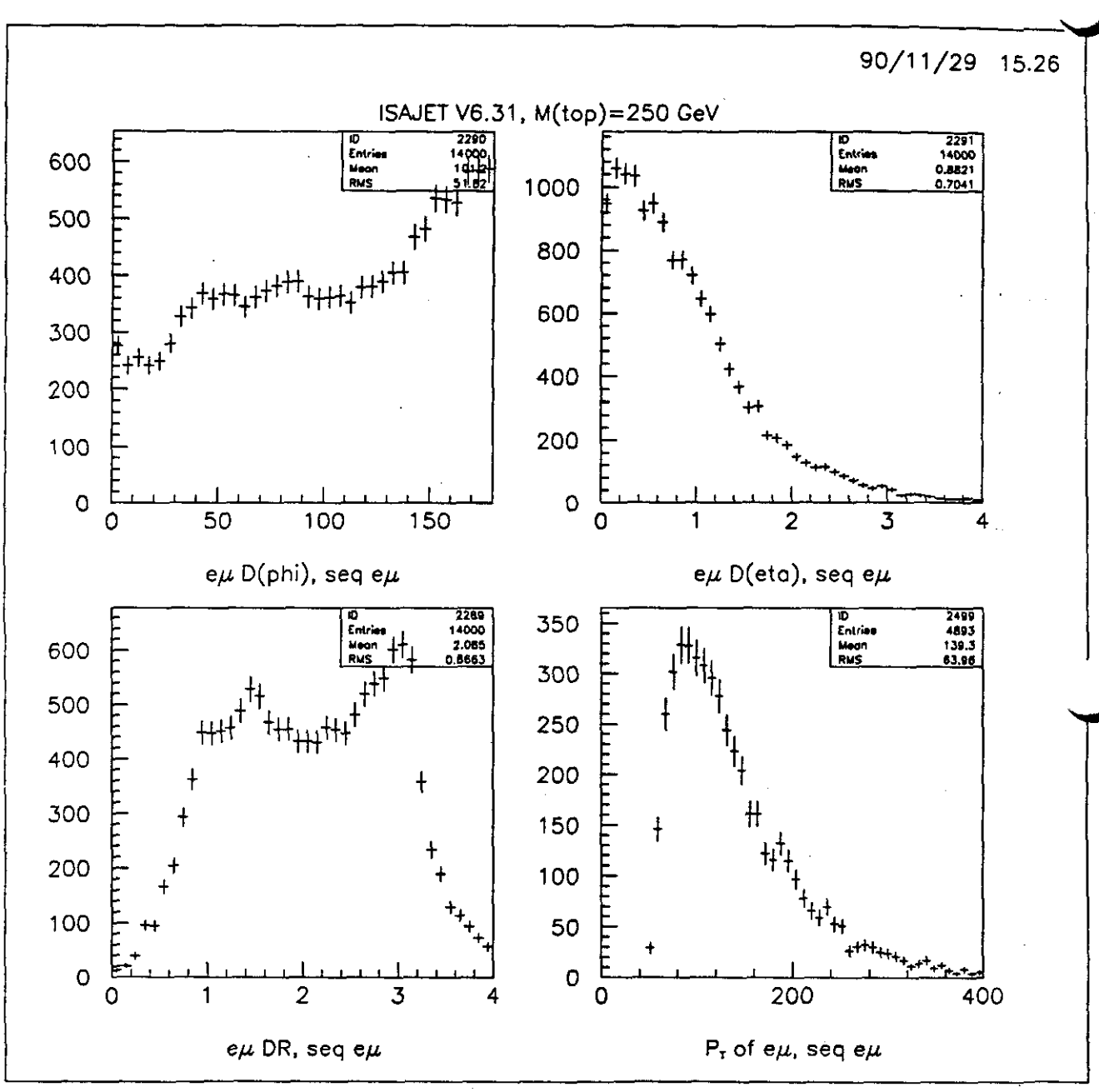

Figure 11) Properties of the $e\mu$ pairs obtained from all $e\mu$ combinations found in the events: a) $\Delta\phi$; b) $\Delta\eta$; c) ΔR; and d) the p_t distribution of all the $e\mu$ pairs. Lepton cuts are as in Figure [8], and in d) we have added the $\Delta\phi > 80$ ° cut.

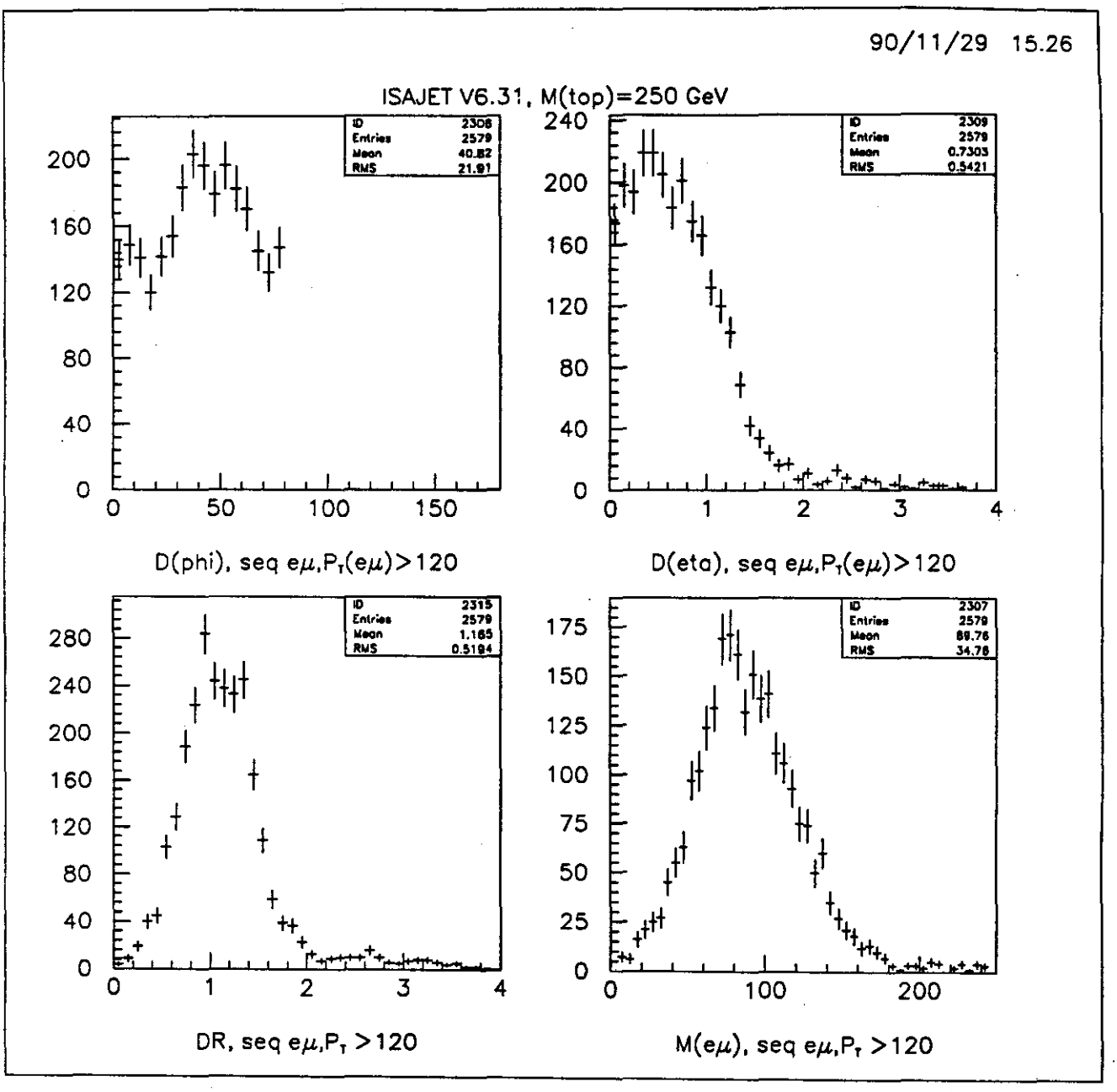

Figure 12) Properties of sequential $e\mu$ pairs after all cuts: a) $\Delta\phi$; b) $\Delta\eta$; c) ΔR; and d) the $e\mu$ invariant mass. In d) we have added the requirement $p_t(e\mu) > 120\ GeV$.

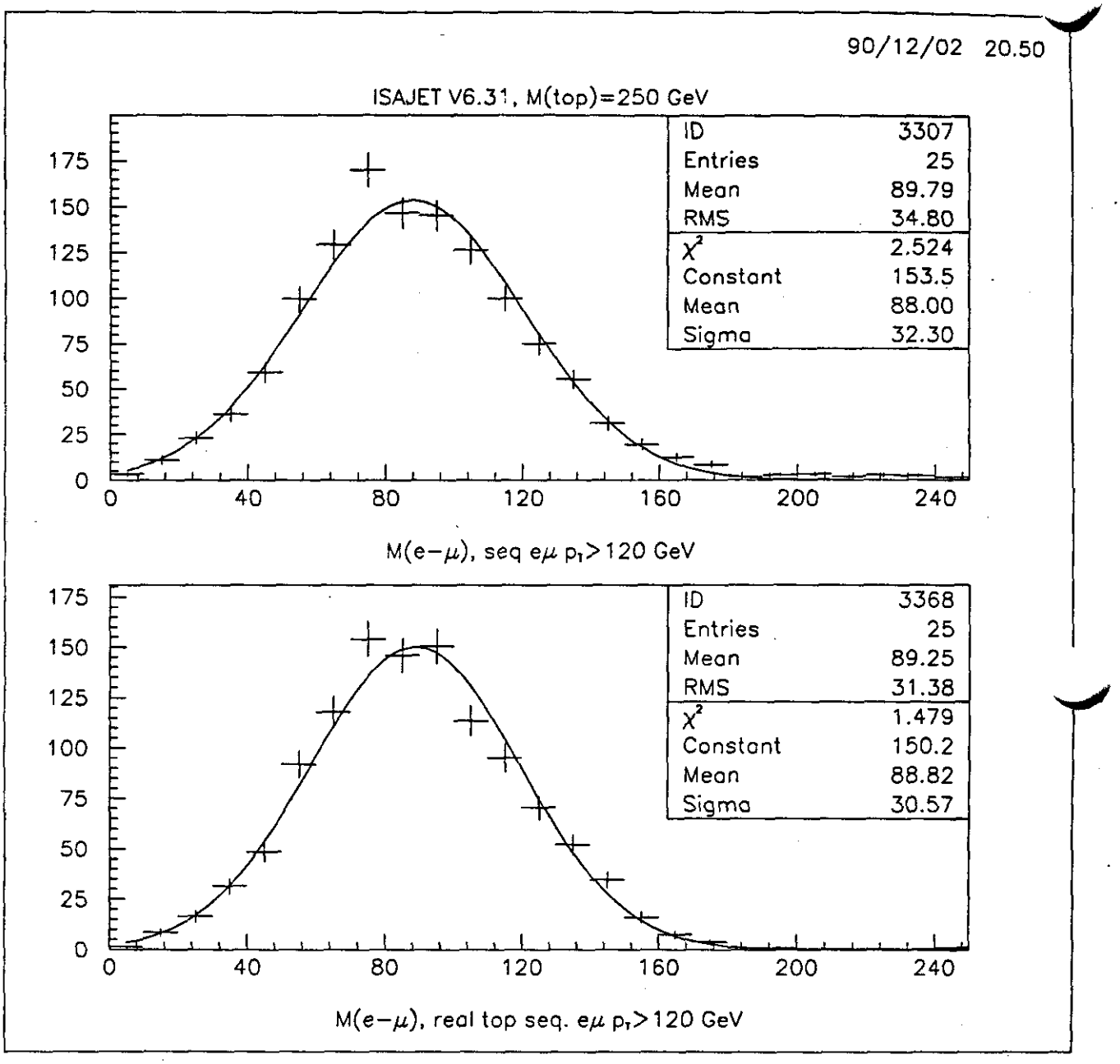

Figure 13) The $e\mu$ invariant mass: a) all $e\mu$ combinations; and b) $e\mu$ combinations that come from real top. The cuts discussed in section 3 are applied in both cases.

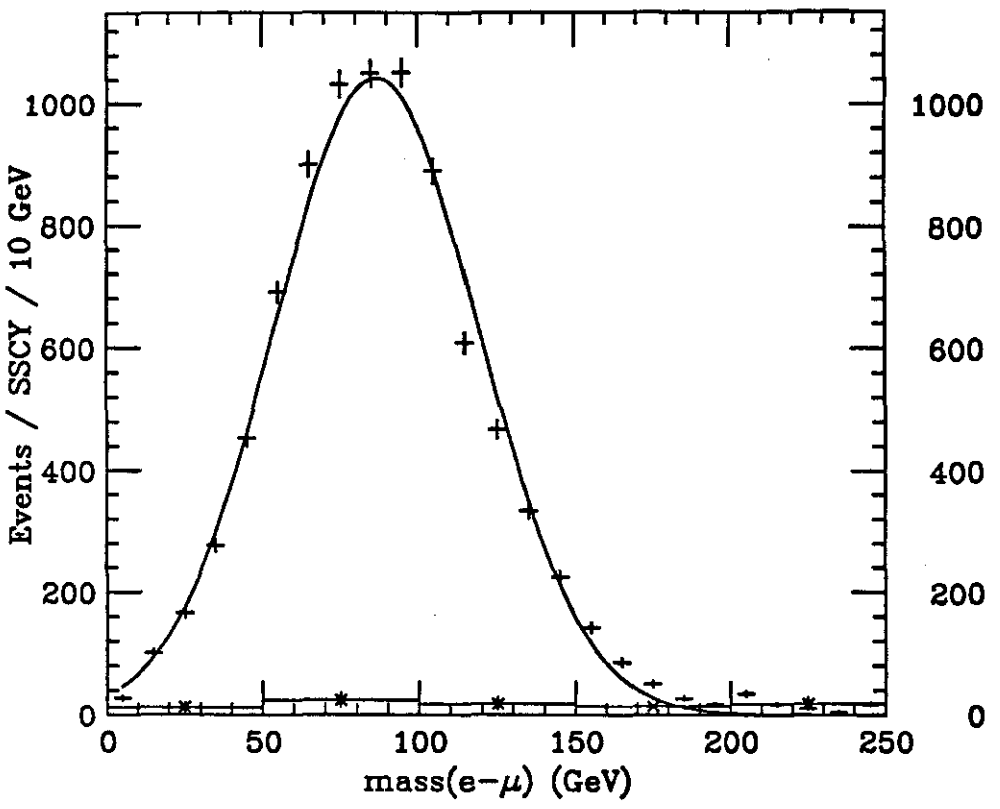

Figure 14) The background to the $e\mu$ invariant mass coming from $Wb\bar{b}$ events is shown under the distribution obtained for $M(top) = 250\ GeV$. The errors on the $Wb\bar{b}$ background are due to Monte Carlo statistics only.

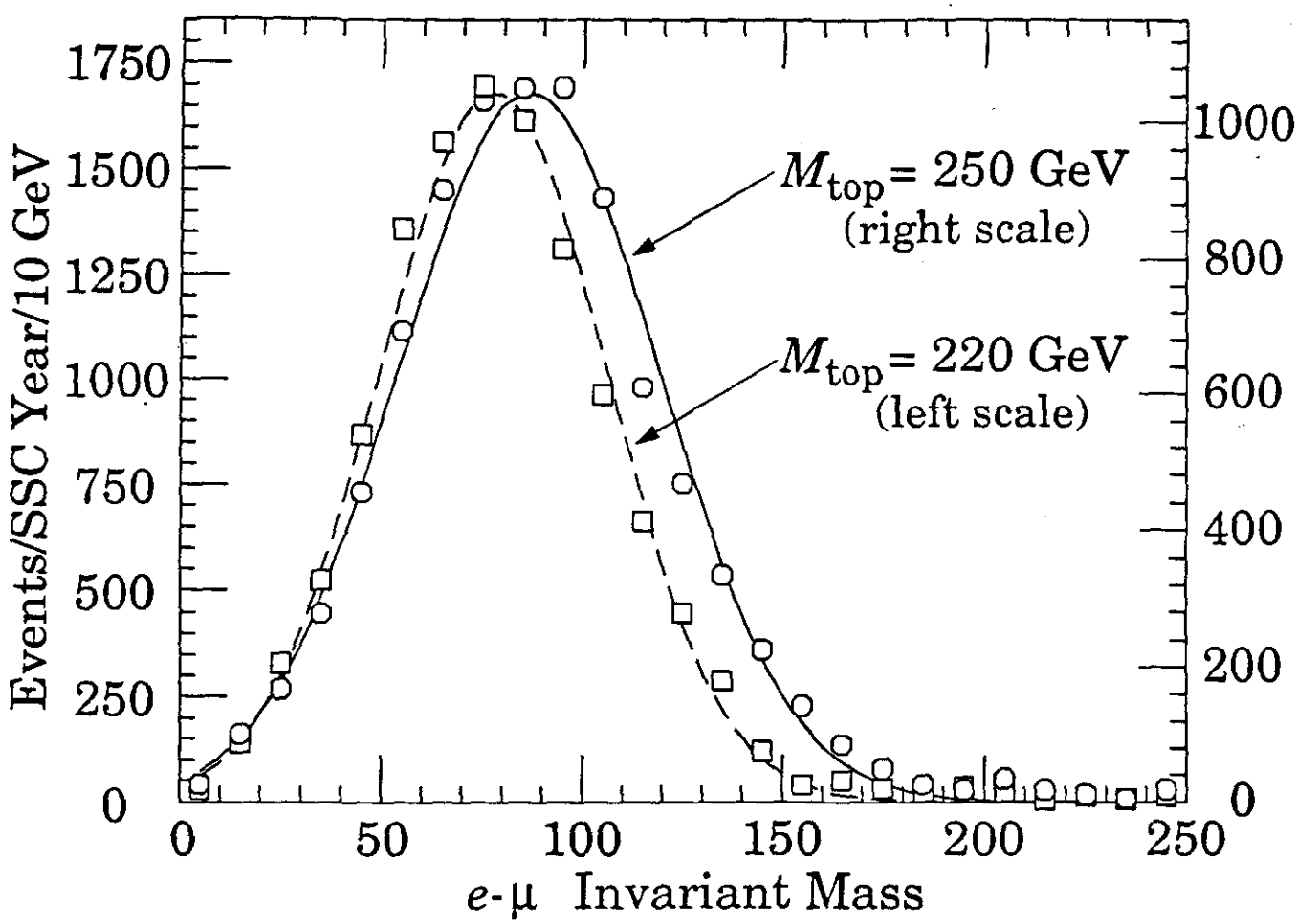

Figure 15) Comparison of the $e\mu$ invariant mass distributions obtained with top masses of 220 and 250 GeV. Both fits are to gaussian shapes.

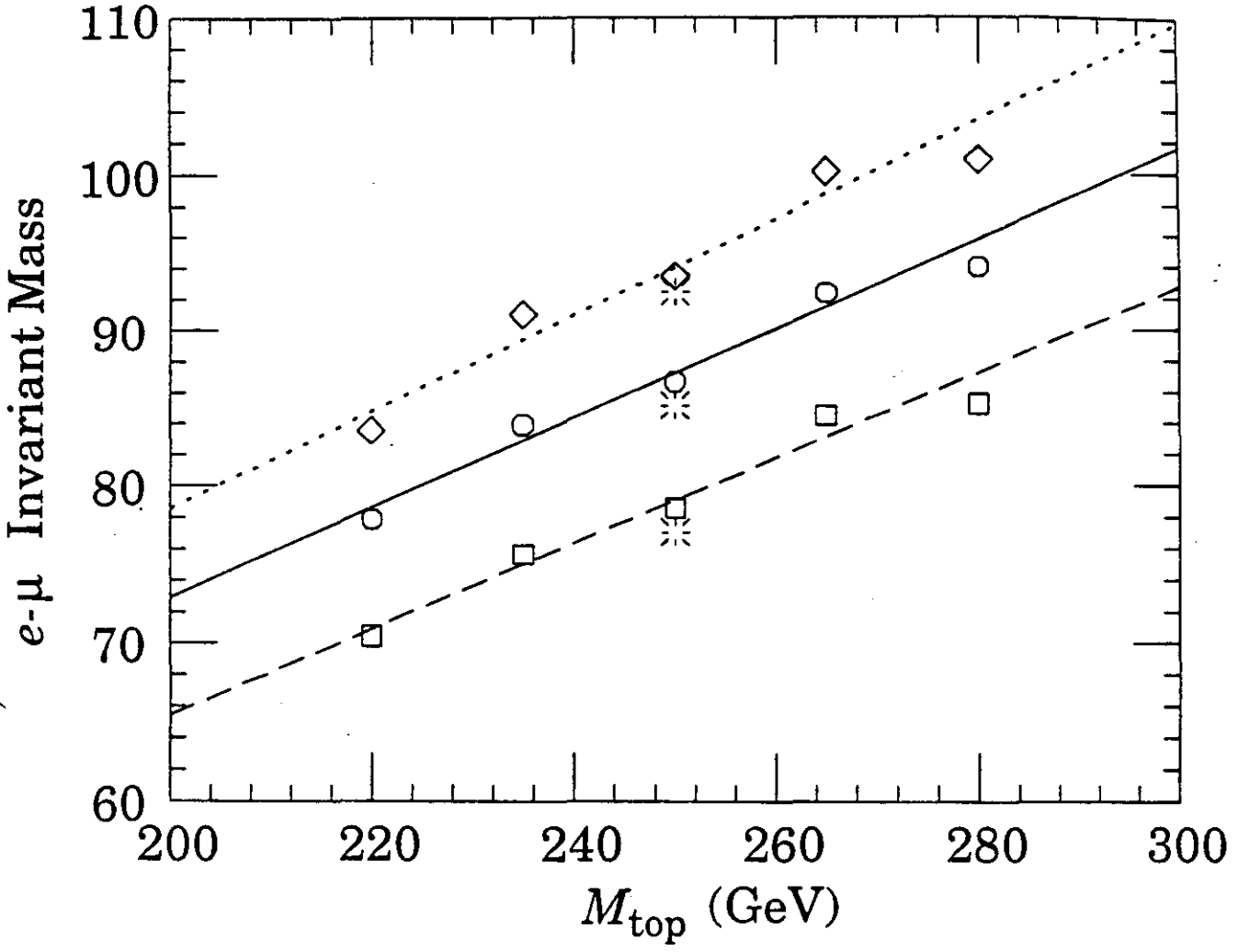

Figure 16) The peak values of the $e\mu$ pair invariant mass as a function of the top mass for different $p_t(e\mu)$ cuts. The extra points at $M(top) = 250\ GeV$ correspond to changing the b fragmentation function by one standard deviation (see section 6).

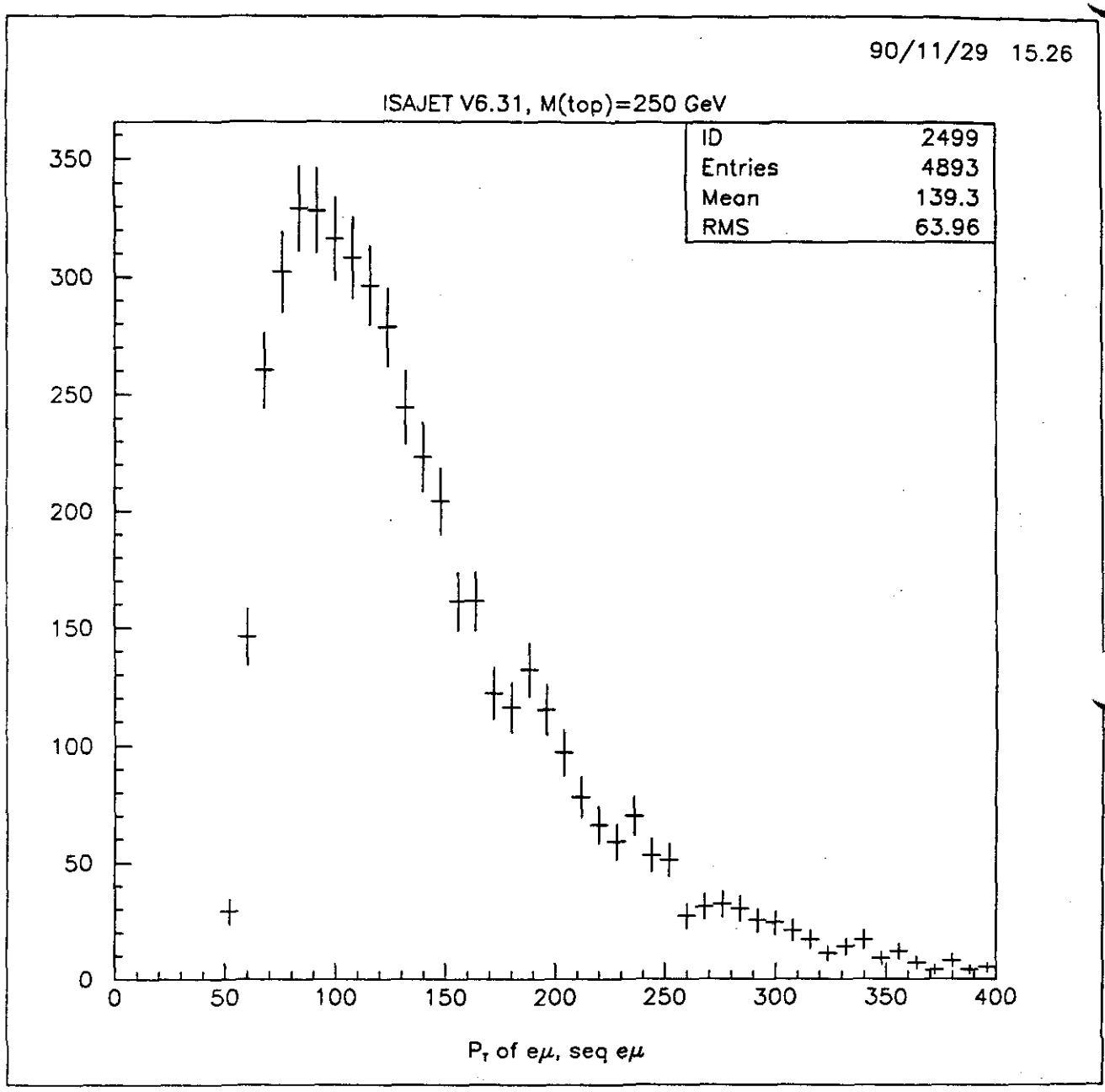

Figure 17) The p_t distribution for all $e\mu$ pairs which pass our cuts.

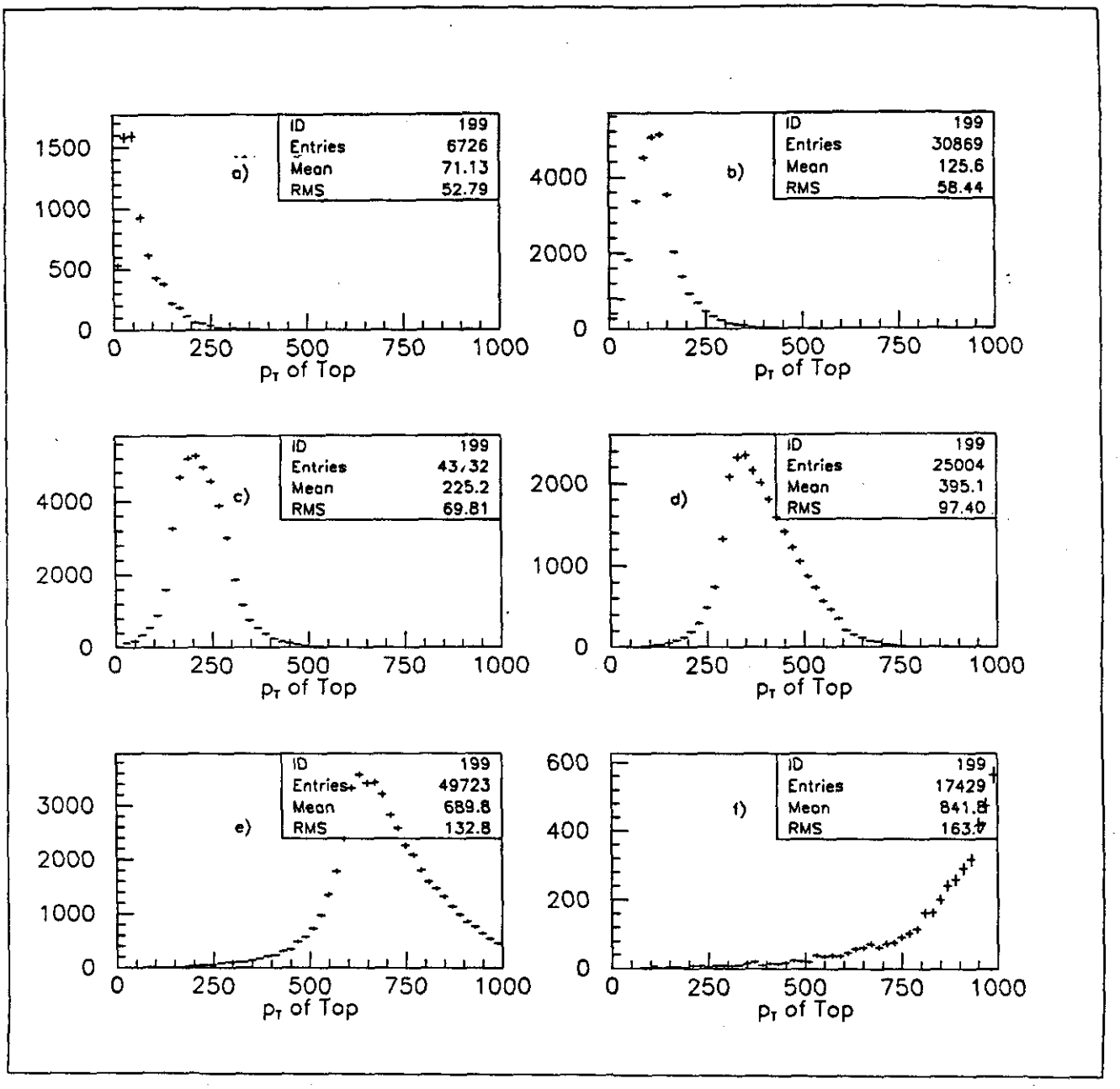

Figure 18) The p_t(top) distribution as obtained by generating events in ISAJET in p_t bins: a) $4 < p_t(\text{top}) < 50\ GeV/c$; b) $50 < p_t(\text{top}) < 150\ GeV/c$; c) $150 < p_t(\text{top}) < 300\ GeV/c$; d) $300 < p_t(\text{top}) < 600\ GeV/c$; e) $600 < p_t(\text{top}) < 1000\ GeV/c$; and f) $1000 < p_t(\text{top}) < 3000\ GeV/c$. Due to choice of binning, in f) only part of the distribution is shown. These runs were made for $M(top) = 250\ GeV$.

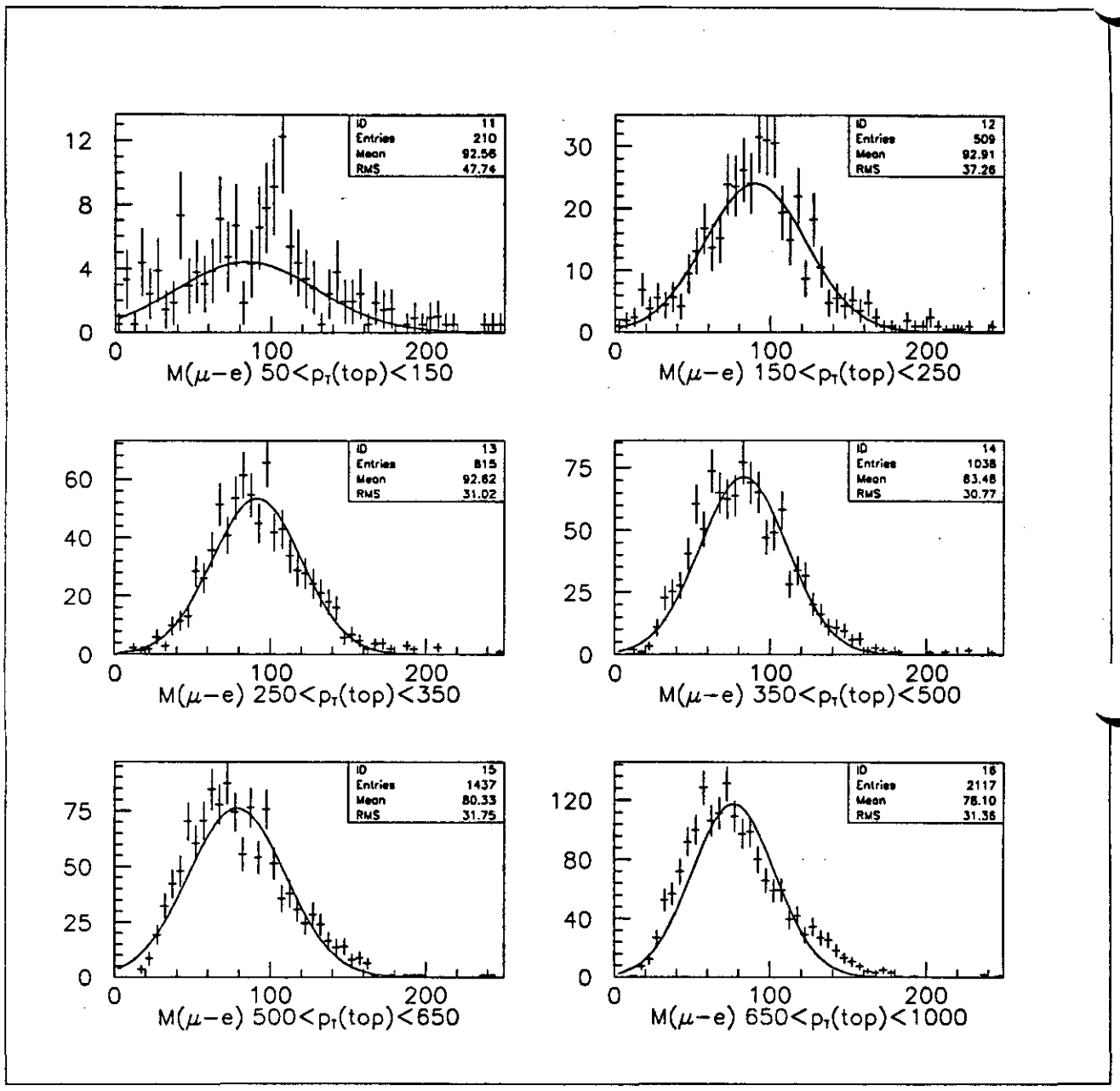

Figure 19) The $e\mu$ invariant mass distribution for $M(top) = 250\ GeV$ in several top p_t ranges: a) $50 < p_t(\text{top}) < 150\ GeV/c$; b) $150 < p_t(\text{top}) < 250\ GeV/c$; c) $250 < p_t(\text{top}) < 350\ GeV/c$; d) $350 < p_t(\text{top}) < 500\ GeV/c$; e) $500 < p_t(\text{top}) < 650\ GeV/c$; and f) $650 < p_t(\text{top}) < 1000\ GeV/c$.

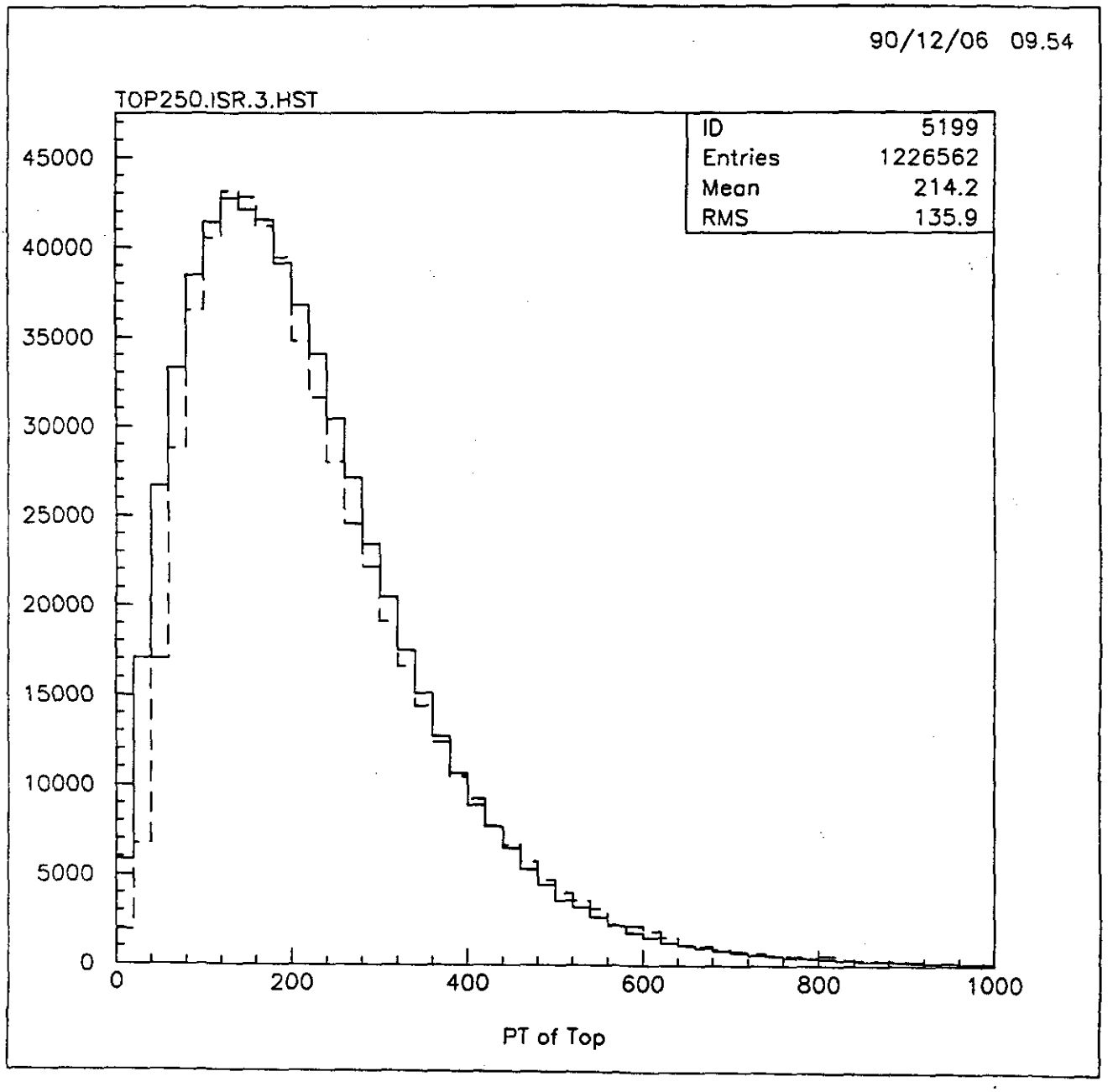

Figure 20) The $p_t(top)$ spectrum before (solid line) and after (dashed line) changing the initial state radiation.

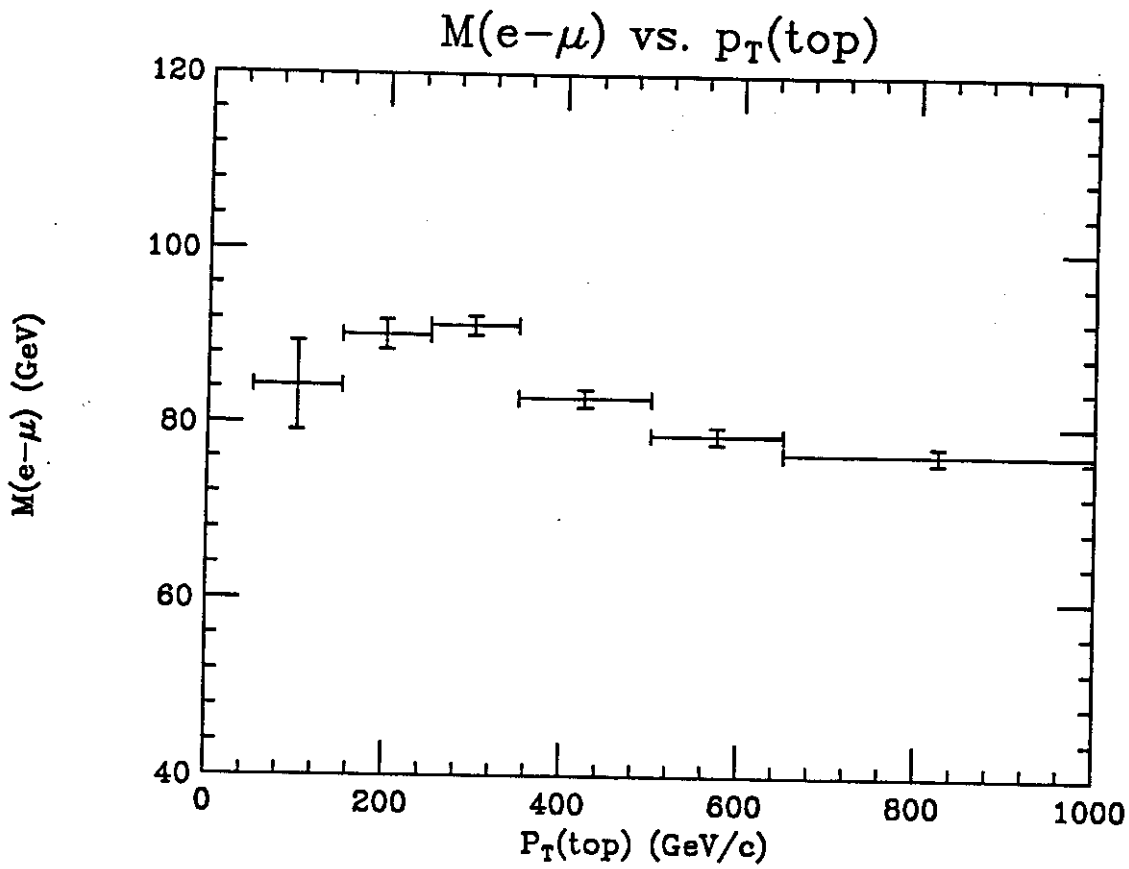

Figure 21) The fitted value of $M(e\mu)$ as a function of the top p_t.

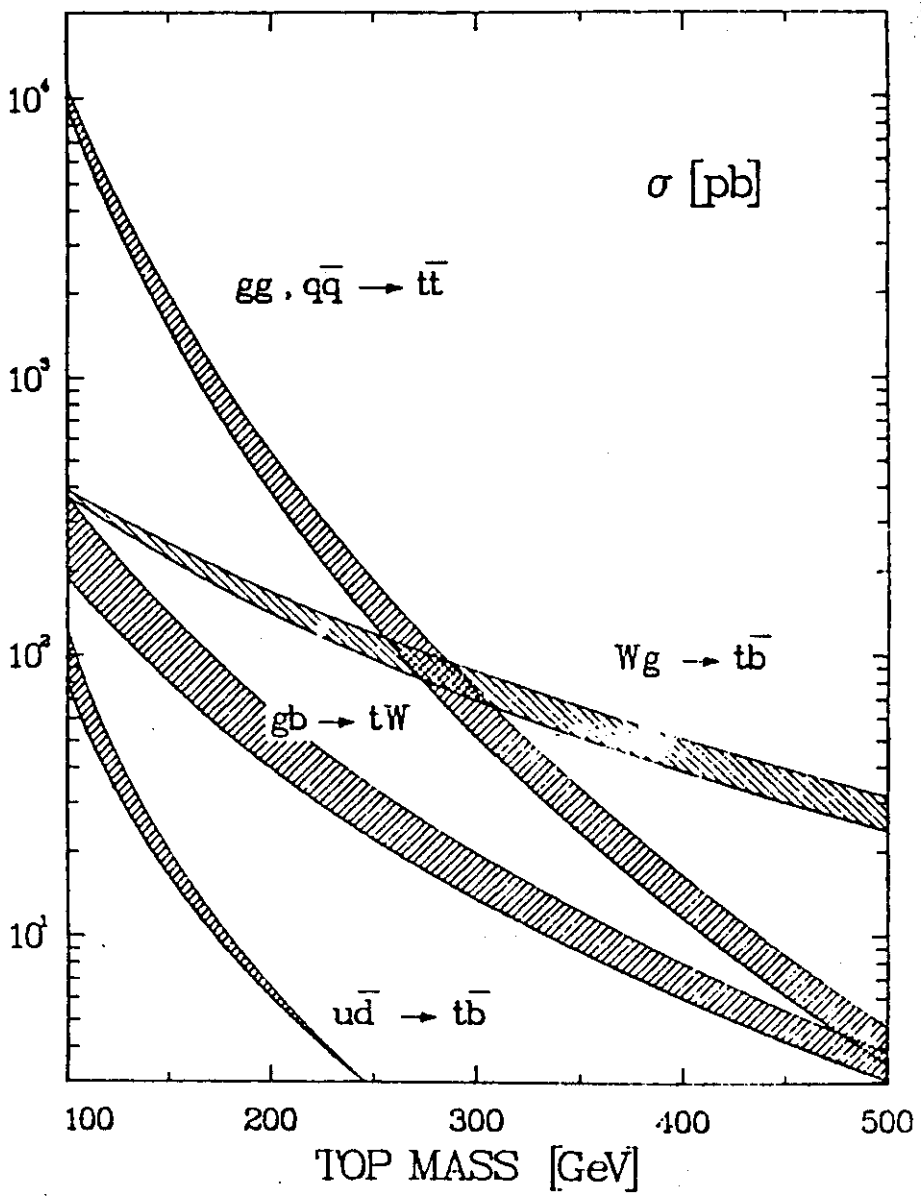

Figure 22) The Wt cross section [10] compared to the $t\bar{t}$ cross section as a function of the top mass at the LHC energy of 16 GeV. The cross section units are pb.